

This article was downloaded by:

On: 23 January 2011

Access details: *Access Details: Free Access*

Publisher *Taylor & Francis*

Informa Ltd Registered in England and Wales Registered Number: 1072954 Registered office: Mortimer House, 37-41 Mortimer Street, London W1T 3JH, UK



Journal of Coordination Chemistry

Publication details, including instructions for authors and subscription information:

<http://www.informaworld.com/smpp/title~content=t713455674>

Syntheses, Crystal Structures, Superoxide Dismutase-Like Behaviors and Physical Properties of Four Manganese(III) Complexes with Di-Schiff Bases Derived from Salicylaldehyde and Polyamines

Hai-Liang Zhu^a; Ye-Xiang Tong^a; Xiao-Lan Yu^a; Xiao-Ming Chen^a

^a School of Chemistry and Chemical Engineering, Zhongshan University, Guangzhou, China

Online publication date: 15 September 2010

To cite this Article Zhu, Hai-Liang , Tong, Ye-Xiang , Yu, Xiao-Lan and Chen, Xiao-Ming(2002) 'Syntheses, Crystal Structures, Superoxide Dismutase-Like Behaviors and Physical Properties of Four Manganese(III) Complexes with Di-Schiff Bases Derived from Salicylaldehyde and Polyamines', *Journal of Coordination Chemistry*, 55: 7, 843 – 852

To link to this Article: DOI: 10.1080/0095897022000001593

URL: <http://dx.doi.org/10.1080/0095897022000001593>

PLEASE SCROLL DOWN FOR ARTICLE

Full terms and conditions of use: <http://www.informaworld.com/terms-and-conditions-of-access.pdf>

This article may be used for research, teaching and private study purposes. Any substantial or systematic reproduction, re-distribution, re-selling, loan or sub-licensing, systematic supply or distribution in any form to anyone is expressly forbidden.

The publisher does not give any warranty express or implied or make any representation that the contents will be complete or accurate or up to date. The accuracy of any instructions, formulae and drug doses should be independently verified with primary sources. The publisher shall not be liable for any loss, actions, claims, proceedings, demand or costs or damages whatsoever or howsoever caused arising directly or indirectly in connection with or arising out of the use of this material.

SYNTHESES, CRYSTAL STRUCTURES, SUPEROXIDE DISMUTASE-LIKE BEHAVIORS AND PHYSICAL PROPERTIES OF FOUR MANGANESE(III) COMPLEXES WITH DI-SCHIFF BASES DERIVED FROM SALICYLALDEHYDE AND POLYAMINES

HAI-LIANG ZHU, YE-XIANG TONG,
XIAO-LAN YU and XIAO-MING CHEN*

*School of Chemistry and Chemical Engineering, Zhongshan University,
Guangzhou 510275, China*

(Received 7 December 2000; Revised 18 April 2001; In final form 24 September 2001)

Four manganese(III) complexes, [Mn(salMeDPT)(O₂CMe)] **1**, [Mn(salMeDPT)Cl] · MeCN **2**, [Mn(salEDPA)Cl] **3** and [Mn(salEDPA)](MeCO₂) **4** have been prepared, where the di-Schiff-base salMeDPT and salEDPA were from the (2 + 1) condensation of salicylaldehyde with 4-methyl-4-azaheptane-1,7-diamine and with 4,7-diazadecane-1,10-diamine, respectively. The four complexes have been characterized by elemental analyses and cyclic voltammetry, while complexes **1–3** have also been characterized by single-crystal x-ray diffraction, which reveals all the Mn(III) atoms in these complexes adopt slightly compressed octahedra with the Mn–O and Mn–N bond lengths in ranges 1.882(3)–1.890(3) and 2.021(4)–0.546(4) Å, respectively. The results of activity assay indicate that complexes **1–4** have moderate superoxide dismutase activities.

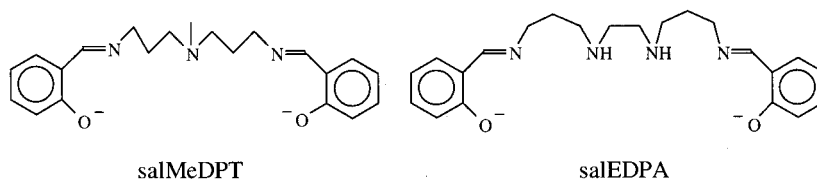
Keywords: Manganese(III) complexes; Di-Schiff base; Crystal structure; SOD activity; Electrochemical properties

INTRODUCTION

Superoxide radical anion, a product of cellular respiration, has been demonstrated to be a mediator of ischemia reperfusion injury, inflammatory diseases, and vascular diseases [1–3]. The main line of defense in mammalian organisms for controlling extracellular and intracellular superoxide radical anions are the CuZn-, Mn- and Fe-containing superoxide dismutase (SOD) [4]. SOD catalyzes the dismutation of superoxide ion to the non-radical products oxygen and hydrogen peroxide [5] and protects living cells against the toxicity of hyperoxia and against the dioxygen-dependent toxicities [6] of viologens, quinones, hypervalent compounds, and benzofurazans. Recently, the application of SOD as a pharmaceutical has attracted much attention [7]. Since there are problems, such as the cost, bioavailability, stability and immunogenicity, associated

*Corresponding author. Fax: 86 20 84112245. E-mail: cesxm@zsu.edu.cn

with using an enzyme as a pharmaceutical, stable, nontoxic, low-molecular-weight metal complexes of SOD might be able to substitute for SOD in such applications, with desirable qualities, low cost, cell permeability, and nonimmunogenicity. The crystal structures [8] of native MnSOD from *Escherichia coli*, *Thermus thermophilus* and human mitochondria have been determined, showing high homology between the bacterial and the eukaryotic MnSOD and confirming that in each case the Mn(III) ion has five ligands (three histidines, one aspartate, and one hydroxide ion) with a distorted trigonal-bipyramidal geometry. Several manganese(II) and manganese(III) complexes have been reported to show SOD activity, independent of the coordination numbers around the metal atoms [9,10]. In this paper we describe the synthesis, characterization and SOD-like activity of four monomeric manganese(III) complexes with two di-Schiff bases, salMeDPT and salEDPA (as shown in the following scheme).



EXPERIMENTAL

Materials

Reagents and solvents used were of commercially available reagent quality. The di-Schiff base salMeDPT (or salEDPA) was prepared by the (2 + 1) condensation of salicylaldehyde with 4-methyl-4-azaheptane-1,7-diamine or 4,7-diazadecane-1,10-diamine in acetonitrile at room temperature. Further isolation was not carried out and the ligand solution was subsequently used for the preparation of the metal complexes.

Physical Techniques

The C, H and N elemental analyses were carried out with a Perkin-Elmer 240Q elemental analyzer. The cyclic voltammograms were measured from 2.0 to -2.0 V at room temperature, with a sample concentration of 1.0×10^{-4} M in MeCN solution containing Bu_4NPF_6 (0.1 M) and a scan speed of 100 mV s^{-1} . A platinum wire working electrode, a platinum plate auxiliary electrode and a saturated calomel electrode (SCE) reference electrode were employed. All potentials were measured with respect to SCE and the experiments were carried out at *ca.* 20°C . The magnetic susceptibility data were obtained on polycrystalline samples at 280 K in a magnetic field of 0.5 T after zero-field cooling using a SQUID magnetometer.

SOD Activity Determination

The SOD activities were evaluated by the classical nitro blue tetrazolium (NBT) assay [11]. The reduction of NBT was monitored at 560 nm on a Shimadzu UV-240 spectrophotometer. All photo-induced reactions were performed at 30°C .

Preparations of Metal Complexes

[Mn(salMeDPT)(O₂CMe)] **1** To a methanol solution (5 mL) of Mn(O₂CMe)₂ · 4H₂O (245 mg, 1 mmol) was added an acetonitrile solution (3 mL) of salMeDPT (1 mmol) with stirring for 30 min. Upon slow diffusion of diethyl ether into the resulting dark brown solution for two days, large black prismatic crystals of complex **1** were deposited and collected by filtration, washed with methanol, acetonitrile and diethyl ether and dried in a vacuum desiccator over silica gel (yield 81%). Anal. calcd. for C₂₃H₂₈N₃O₄Mn(%): C, 59.35; H, 6.06; N, 9.03. Found: C, 60.00; H, 6.01; N, 9.11.

[Mn(salMeDPT)Cl] · MeCN **2** Complex **2** was prepared as for complex **1** using MnCl₂ · 4H₂O in place of Mn(O₂CMe)₂ · 4H₂O. The large black prismatic crystals of complex **2** were obtained (yield 83%). Anal. calcd. for C₂₃H₂₈N₄O₂ClMn(%): C, 57.21; H, 5.84; N, 11.60. Found: C, 57.25; H, 5.65; N, 11.68.

[Mn(salEDPA)Cl] **3** To a methanol solution (5 mL) of MnCl₂ · 4H₂O (198 mg, 1 mmol) was added an acetonitrile solution (3 mL) of salEDPA (1 mmol) with stirring for 30 min. Upon slow diffusion of diethyl ether into the resulting dark brown solution for 24 h, large black prismatic crystals of complex **3** were deposited and collected by filtration, sequentially washed with methanol, acetonitrile and diethyl ether and dried in a vacuum desiccator over silica gel (yield 81%). Anal. calcd. for C₂₂H₂₈N₄O₂Cl Mn(%): C, 56.12; H, 5.99; N, 11.90. Found: C, 56.36; H, 5.95; N, 12.05.

[Mn(salEDPA)](MeCO₂) **4** Complex **4** was prepared as for complex **3** using Mn(MeCO₂)₂ · 4H₂O in place of MnCl₂ · 4H₂O. The dark-red, long-needle, crystals of complex **4** were obtained (yield 85%). Anal. calcd. for C₂₄H₃₁N₄O₄Mn(%): C, 58.30; H, 6.32; N, 11.33. Found: C, 58.31; H, 6.22; N, 11.23.

X-ray Crystallography

Diffraction intensities for complexes **1**, **2** and **3** were collected at 293(2) K on a Siemens R3m diffractometer using Mo-*K* α radiation ($\lambda = 0.71073 \text{ \AA}$). Lorentz-polarization and absorption corrections were applied [12]. The structure solutions and full-matrix least-squares refinements based on F^2 were performed with the SHELXS-97 [13] and SHELXL-97 [14] program packages, respectively. All the non-hydrogen atoms were refined anisotropically. Hydrogen atoms were generated geometrically and fixed on their parent carbon atoms, and assigned isotropic thermal parameters and included in the structure-factor calculations. Analytical expressions of neutral-atom scattering factors were employed, and anomalous dispersion corrections were incorporated [15]. The crystallographic data for the complexes are summarized in Table I. The non-hydrogen atomic coordinates and selected bond lengths and bond angles for the complexes are presented in Tables II and III, respectively. Additional crystallographic data are available as supplementary data.

RESULTS AND DISCUSSION

Structure Description

[Mn(salMeDPT)(O₂CMe)] **1** and *[Mn(salMeDPT)Cl] · MeCN* **2** Complexes **1** and **2** exist as discrete molecules in the solid state, and the molecular structures of

TABLE I Crystal data^a for complexes **1**, **2** and **3**

Complex	1	2	3
Formula	C ₂₃ H ₂₈ MnN ₃ O ₄	C ₂₁ H ₂₅ ClMnN ₃ O ₂	C ₂₂ H ₂₈ ClMnN ₄ O ₂
Fw	465.42	441.84	470.87
space group	<i>P2₁/n</i>	<i>P1</i>	<i>Pccn</i>
<i>a</i> (Å)	9.457(4)	9.323(2)	7.775(4)
<i>b</i> (Å)	19.229(5)	10.824(3)	16.078(7)
<i>c</i> (Å)	11.988(5)	12.671(5)	17.437(13)
α (deg)	90	111.590(10)	90
β (deg)	92.51(1)	99.960(10)	90
γ (deg)	90	90.060(10)	90
<i>V</i> (Å ³)	2178(1)	1168.1(6)	2180(2)
<i>Z</i>	4	2	4
λ (MoK α) (Å)	0.71073	0.71073	0.71073
<i>T</i> (K)	293	293	293
ρ (g/cm ³)	1.419	1.312	1.435
μ (MoK α) (cm ⁻¹)	0.641	0.702	0.755
No. of unique reflections	4272	4601	1807
No. of observed [<i>I</i> = 2 σ (<i>I</i>)]	3215	3350	1389
Crystal size	0.55 × 0.45 × 0.50	0.55 × 0.55 × 0.60	0.65 × 0.40 × 0.60
<i>R</i> ₁ [<i>I</i> > 2 σ (<i>I</i>)] ^a	0.0591	0.0633	0.0366
<i>wR</i> ₂ (all data) ^a	0.0823	0.0915	0.0537

$$^a R_1 = \frac{\sum ||F_o| - |F_c||}{\sum |F_o|}, wR_2 = \left[\frac{\sum w(F_o^2 - F_c^2)^2}{\sum w(F_o^2)^2} \right]^{1/2}.$$

TABLE IIA Fractional atomic coordinates and isotropic thermal parameters (Å² × 10³) for complexes **1–3**

Atom	<i>x/a</i>	<i>y/b</i>	<i>z/c</i>	<i>U</i> _{eq} ^a
Complex 1				
Mn1	0.21962(6)	0.90802(3)	0.19184(5)	0.0287(2)
O3	0.0144(3)	0.8720(2)	0.1428(3)	0.0408(7)
O4	−0.1698(4)	0.8200(2)	0.0596(4)	0.071(1)
C22	−0.0513(5)	0.8184(2)	0.1049(4)	0.0379(9)
C23	0.0234(6)	0.7495(3)	0.1184(5)	0.063(2)
O1	0.1377(3)	0.9447(1)	0.3202(2)	0.0332(6)
O2	0.2977(3)	0.8697(1)	0.0639(2)	0.0365(7)
N1	0.2978(4)	0.8279(2)	0.2901(3)	0.0341(8)
N2	0.4504(4)	0.9618(2)	0.2491(3)	0.0396(8)
N3	0.1944(3)	0.9995(2)	0.1081(3)	0.0298(7)
C1	0.0624(4)	0.9044(2)	0.3851(3)	0.0307(8)
C2	−0.0606(4)	0.9301(2)	0.4295(3)	0.0364(9)
C3	−0.1384(5)	0.8902(2)	0.5011(3)	0.042(1)
C4	−0.0948(5)	0.8244(3)	0.5321(4)	0.044(1)
C5	0.0276(5)	0.7979(2)	0.4915(4)	0.042(1)
C6	0.1065(4)	0.8364(2)	0.4159(3)	0.0334(9)
C7	0.2348(4)	0.8059(2)	0.3758(3)	0.0358(9)
C8	0.4361(5)	0.7979(2)	0.2657(4)	0.042(1)
C9	0.5577(5)	0.8451(3)	0.3038(5)	0.059(1)
C10	0.5646(6)	0.9163(3)	0.2257(7)	0.086(2)
C11	0.4559(7)	0.9889(4)	0.3628(6)	0.085(2)
C12	0.4739(6)	1.0246(3)	0.1751(6)	0.071(2)
C13	0.3699(5)	1.0830(2)	0.1833(5)	0.055(1)
C14	0.2135(5)	1.0645(2)	0.1716(4)	0.0379(9)
C15	0.1718(4)	1.0029(2)	0.0023(3)	0.0309(8)
C16	0.1786(4)	0.9441(2)	−0.0724(3)	0.0299(8)
C17	0.1322(4)	0.9533(2)	−0.1840(3)	0.0348(9)
C18	0.1481(5)	0.9015(2)	−0.2627(4)	0.041(1)
C19	0.2128(5)	0.8397(2)	−0.2300(3)	0.040(1)
C20	0.2614(5)	0.8295(2)	−0.1210(4)	0.039(1)
C21	0.2445(4)	0.8811(2)	−0.0391(3)	0.0298(8)

TABLE IIA *Continued*

Atom	<i>x/a</i>	<i>y/b</i>	<i>z/c</i>	U_{eq}^a
Complex 2				
Mn1	0.16360(7)	0.08410(6)	0.29741(5)	0.0389(2)
Cl1	-0.0920(1)	-0.0319(1)	0.2265(1)	0.0539(3)
O1	0.2450(4)	-0.0820(3)	0.2683(3)	0.0481(8)
O2	0.0784(3)	0.2482(3)	0.3266(2)	0.0433(7)
N1	0.1822(4)	0.1044(4)	0.4644(3)	0.0385(8)
N2	0.4086(4)	0.1972(4)	0.3653(4)	0.0488(9)
N3	0.1947(4)	0.0854(4)	0.1434(3)	0.0455(9)
C1	0.2068(5)	-0.1712(4)	0.3107(4)	0.042(1)
C2	0.2138(6)	-0.3061(5)	0.2476(5)	0.058(1)
C3	0.1789(6)	-0.4015(5)	0.2892(5)	0.061(1)
C4	0.1388(6)	-0.3645(5)	0.3969(5)	0.059(1)
C5	0.1348(5)	-0.2321(5)	0.4619(4)	0.047(1)
C6	0.1667(4)	-0.1331(5)	0.4204(4)	0.0401(9)
C7	0.1734(5)	0.0050(5)	0.4968(4)	0.042(1)
C8	0.2213(5)	0.2387(5)	0.5538(4)	0.046(1)
C9	0.3860(6)	0.2703(6)	0.5781(5)	0.063(2)
C10	0.4666(6)	0.1976(7)	0.4844(5)	0.069(2)
C11	0.4107(7)	0.3395(6)	0.3765(7)	0.083(2)
C12	0.5068(6)	0.1235(7)	0.2929(6)	0.081(2)
C13	0.4623(7)	0.1107(6)	0.1617(5)	0.071(2)
C14	0.3232(6)	0.0232(5)	0.0970(4)	0.058(1)
C15	0.1133(6)	0.1456(5)	0.0880(4)	0.051(1)
C16	-0.0017(5)	0.2264(5)	0.1298(4)	0.047(1)
C17	-0.0988(7)	0.2646(6)	0.0509(5)	0.069(2)
C18	-0.2118(8)	0.3412(7)	0.0855(5)	0.082(2)
C19	-0.2274(7)	0.3864(6)	0.2015(5)	0.070(2)
C20	-0.1294(6)	0.3548(5)	0.2808(4)	0.052(1)
C21	-0.0150(5)	0.2738(4)	0.2467(4)	0.042(1)
N4	0.398(2)	-0.581(1)	0.092(1)	0.096(4)
C22	0.370(2)	-0.630(1)	0.005(1)	0.086(4)
C23	0.360(3)	-0.699(2)	-0.115(1)	0.159(9)
Complex 3				
Mn1	0.2500	0.7500	0.45838(3)	0.0356(2)
Cl1	-0.2500	0.7500	0.64491(6)	0.0568(3)
O1	0.1487(2)	0.8559(1)	0.46037(9)	0.0437(5)
N2	0.0926(3)	0.7067(1)	0.5485(1)	0.0437(6)
C1	0.0840(4)	0.8961(2)	0.4004(1)	0.0383(6)
N1	0.0624(3)	0.7156(1)	0.38410(1)	0.0420(5)
C2	0.0864(4)	0.9833(2)	0.4003(2)	0.0500(7)
C10	0.0138(4)	0.6234(2)	0.5369(2)	0.0561(8)
C5	-0.0666(4)	0.9024(2)	0.2786(2)	0.0526(8)
C9	-0.1007(4)	0.6207(2)	0.4666(2)	0.0586(9)
C6	0.0082(3)	0.8553(2)	0.3377(1)	0.0398(6)
C4	-0.0606(4)	0.9874(2)	0.2797(2)	0.0601(9)
C7	-0.0130(4)	0.7658(2)	0.3378(1)	0.0448(7)
C3	0.0181(4)	1.0276(2)	0.3401(2)	0.0566(8)
C8	-0.0082(4)	0.6305(2)	0.3900(2)	0.0509(8)
C11	0.1996(4)	0.7099(2)	0.6180(2)	0.0589(9)

complexes **1** and **2** are shown in Figs. 1 and 2, respectively. In these two complexes, the Mn(III) atom is six-coordinated in an elongated octahedron with three nitrogen and two oxygen atoms from the salMeDPT ligand, and one acetate oxygen atom and one chloro atom in complexes **1** and **2**, respectively. The most distorted bond angles of the coordination polyhedra are the N(1)–Mn(1)–N(3) angles at 164.1(1) and

TABLE IIB Selected bond lengths (Å) and angles (°) for **1**, **2** and **3**

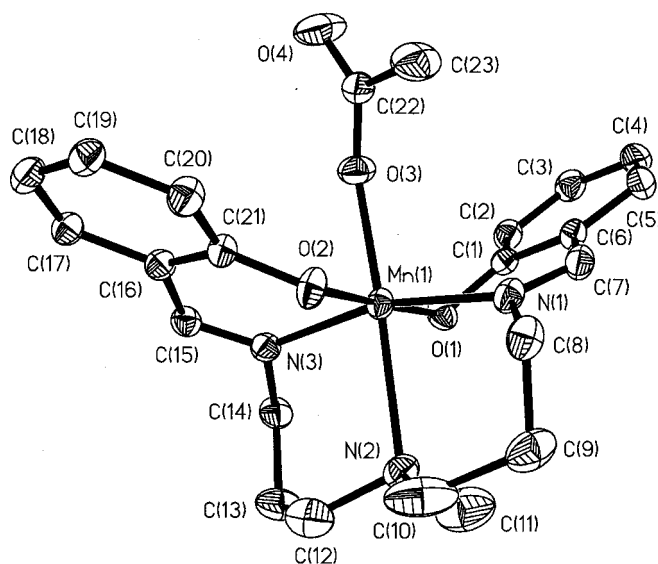
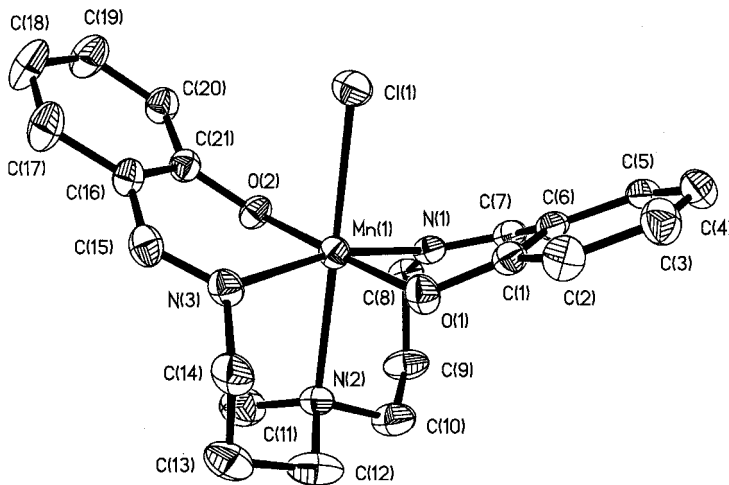
1			
Mn(1)–O(2)	1.882(3)	Mn(1)–O(1)	1.890(3)
Mn(1)–N(3)	2.034(3)	Mn(1)–N(1)	2.057(3)
Mn(1)–O(3)	2.120(3)	Mn(1)–N(2)	2.485(4)
O(2)–Mn(1)–O(1)	178.6(1)	O(2)–Mn(1)–N(3)	88.8(1)
O(1)–Mn(1)–N(3)	92.0(1)	O(2)–Mn(1)–N(1)	91.7(1)
O(1)–Mn(1)–N(1)	87.9(1)	N(3)–Mn(1)–N(1)	164.1(1)
O(2)–Mn(1)–O(3)	91.9(1)	O(1)–Mn(1)–O(3)	86.9(1)
N(3)–Mn(1)–O(3)	93.4(1)	N(1)–Mn(1)–O(3)	102.5(1)
O(2)–Mn(1)–N(2)	91.0(1)	O(1)–Mn(1)–N(2)	90.4(1)
N(3)–Mn(1)–N(2)	81.9(1)	N(1)–Mn(1)–N(2)	82.2(1)
O(3)–Mn(1)–N(2)	174.5(1)		
2			
Mn(1)–O(2)	1.882(3)	Mn(1)–O(1)	1.886(2)
Mn(1)–N(1)	2.021(4)	Mn(1)–N(3)	2.027(4)
Mn(1)–N(2)	2.449(4)	Mn(1)–Cl(1)	2.546(1)
O(2)–Mn(1)–O(1)	178.7(1)	O(2)–Mn(1)–N(1)	91.5(1)
O(1)–Mn(1)–N(1)	88.2(1)	O(2)–Mn(1)–N(3)	89.1(1)
O(1)–Mn(1)–N(3)	91.5(1)	N(1)–Mn(1)–N(3)	166.1(1)
O(2)–Mn(1)–N(2)	91.0(1)	O(1)–Mn(1)–N(2)	90.2(1)
N(1)–Mn(1)–N(2)	83.1(1)	N(3)–Mn(1)–N(2)	83.0(2)
O(2)–Mn(1)–Cl(1)	88.6(1)	O(1)–Mn(1)–Cl(1)	90.3(1)
N(1)–Mn(1)–Cl(1)	97.1(1)	N(3)–Mn(1)–Cl(1)	96.8(1)
N(2)–Mn(1)–Cl(1)	179.5(1)		
3			
Mn(1)–O(1)	1.876(2)	Mn(1)–N(1)	2.028(2)
Mn(1)–N(2)	2.109(2)		
O(1)–Mn(1)–N(1)	87.54(8)	O(1)–Mn(1)–N(1a)	93.81(9)
N(1)–Mn(1)–N(1a)	100.6(1)	O(1)–Mn(1)–N(2a)	85.98(8)
N(1)–Mn(1)–N(2a)	169.42(9)	O(1)–Mn(1)–N(2)	92.44(9)
N(1)–Mn(1)–N(2)	88.2(1)	N(2)–Mn(1)–N(2a)	83.8(1)

Symmetric code for **3**: *a*) 1/5 – *x*, 3/2 – *y*, *z*.

TABLE III The CV data (V) of the four Mn complexes in MeCN at room temperature

Complex	<i>Mn(III)/Mn(II)</i>				<i>Mn(IV)/Mn(III)</i>			
	<i>E_{pc}</i>	<i>E_{pa}</i>	ΔE_p	<i>E_{1/2}</i>	<i>E_{pc}</i>	<i>E_{pa}</i>	ΔE_p	<i>E_{1/2}</i>
1	–0.65	–0.55	0.10	–0.60	0.25	0.32	0.07	0.29
2	–0.67	–0.56	0.11	–0.61	0.26	0.34	0.08	0.30
3	–0.68	–0.56	0.12	–0.62	0.25	0.34	0.09	0.30
4	–0.66	–0.56	0.10	–0.60	0.25	0.35	0.10	0.30

166.1(2)° in complexes **1** and **2**, respectively. The two imine nitrogen atoms (N(1) and N(3) from salMeDPT; Mn–N_{imine} = 2.021(4)–2.057(4) Å) and two phenoxo oxygen atoms (O(1) and O(2); Mn–O = 1.882(3)–1.890(3) Å) constitute the coordination equatorial plane. The amine nitrogen atom of salMeDPT and acetato O(3) atom (for **1**) (or chloro atom for **2**) occupy axial positions with significantly longer bond lengths of 2.458(4) and 2.449(4) Å for the Mn–N, the Mn(1)–O(3) (2.120(3) Å) and Mn–Cl (2.546(1) Å) bonds in complexes **1** and **2**, respectively, than the remaining metal–ligand bonds. The distortion may be attributed to the Jahn–Teller effect of the high-spin Mn(III) atom. In the equatorial plane, the Mn–N bonds are slightly longer than Mn–O bonds due to the larger atomic radius of nitrogen atom.

FIGURE 1 ORTEP view (at 30% probability) of the cation in **1**.FIGURE 2 ORTEP view (at 30% probability) of the cation in **2**.

[Mn(salEDPA)]Cl **3** The crystal structure of complex **3** consists of discrete $[Mn(salEDPA)]^+$ cations and chloride ions. The monomeric cation bears a crystallographic two-fold axis passing through the metal atom. As shown in Fig. 3, the metal atom in the cation is also six-coordinate with six donors of salEDPA, displaying an elongated octahedral geometry similar to those found in complexes **1** and **2**. The four nitrogen atoms occupy the equatorial positions and two oxygen atoms occupy the axial positions. The Mn–O length of 1.876(2) Å is close to those in complexes **1** and **2**. The Mn–N bond lengths (2.028(2) and 2.109(2) Å) are similar to those of the

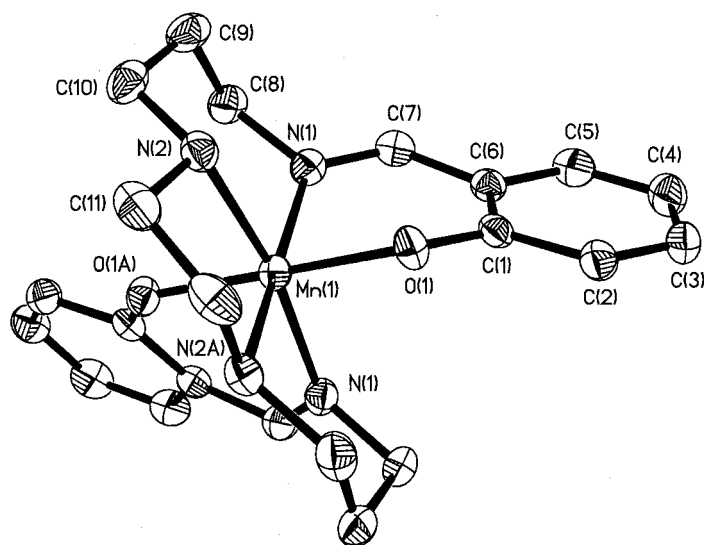


FIGURE 3 ORTEP view (at 30% probability) of the cation in **3**.

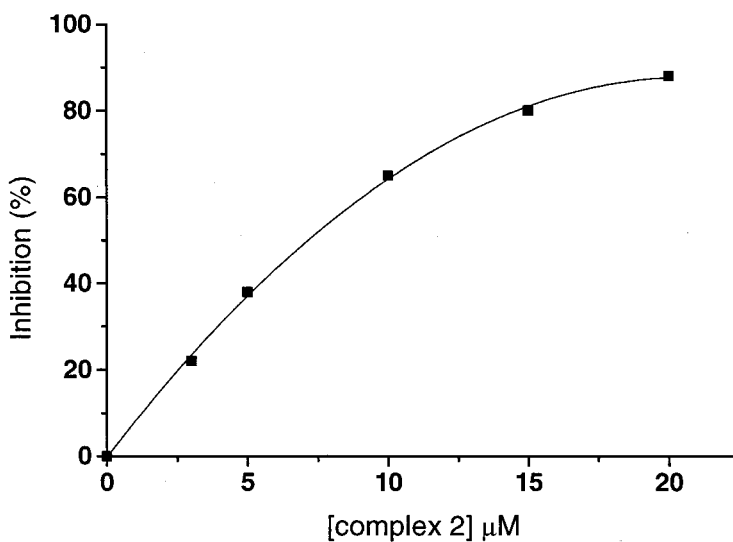


FIGURE 4 The SOD activity of **2** in the riboflavin-methionine-nitro blue tetrazolium assay.

Mn–N_{imine} bonds in complexes **1** and **2**, and much shorter than those of Mn–N_{amine} in complexes **1** and **2**.

SOD-Like Activities

The relationships between the inhibitions (%) and initial concentrations for the four complexes were measured, and that of complex **2** is shown in Fig. 4. The chromophore

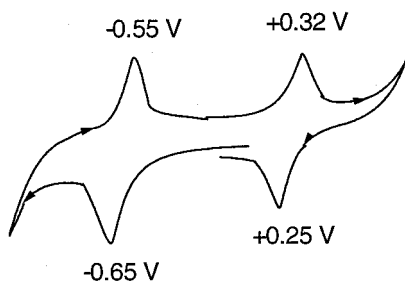


FIGURE 5 Cyclic voltammogram of **1** in MeCN at room temperature with 0.1 M of $\text{Bu}^n_4\text{NPF}_6$ as electrolyte at Pt electrode and SCE reference electrode. Condition: 1.0×10^{-4} M, $\nu = 100 \text{ mV s}^{-1}$.

concentration required to yield 50% inhibition of the reduction of NBT (IC_{50}) was determined by the literature method [11]. The IC_{50} values of complexes **1**, **2**, **3** and **4** are 6.7, 7.6, 6.5 and 7.4 M, respectively, which are approximately nine times higher than the lowest values exhibited by the manganese(II) SOD models $[\text{Mn}(\text{ntb})(\text{Hsal})]\text{ClO}_4$ (ntb = tris(benzimidazol-2-ylmethyl)amine, Hsal = salicylate) ($\text{IC}_{50} = 0.70 \mu\text{M}$) [16] and $\text{Mn}(\text{OBz})(3,5\text{-iPr}_2\text{pzH})(\text{HB}(3,5\text{-iPr}_2\text{pz})_3)$ (OBz = phenol anion, $3,5\text{-iPr}_2\text{pzH}$ = 3,5-diisopropylpyrazole, $\text{HB}(3,5\text{-iPr}_2\text{pz})_3$ = hydrotris(3,5-diisopropyl-1-pyrazolyl)borate) ($\text{IC}_{50} = 0.75 \mu\text{M}$) [17], indicating moderate SOD activities of the four complexes.

Magnetic and Electrochemical Properties

The effective magnetic moments of powder samples for complexes **1–4** at room temperature are 4.75, 4.75, 4.81, 4.76 μ_{B} ($\mu_{\text{B}} \approx 9.27 \times 10^{-24} \text{ J T}^{-1}$), respectively, revealing the trivalent state of Mn(III) ions, which have effective magnetic moments in the range 4.6–4.9 μ_{B} .

The electrochemical properties of the four complexes have been studied by cyclic voltammetry (CV) in dry and degassed MeCN. The free ligands salMEDPT and salEDPA are not electroactive over the range -1.50 V to $+1.50 \text{ V}$. The four complexes are structurally similar and exhibit similar electrochemical behavior. A typical CV for complex **1** is depicted in Fig. 5, and the CV data for the four complexes are presented in Table III. The CV of complex **1** is shown to have two redox waves. The redox couple occurs with the reduction peak at -0.65 V and the corresponding oxidation peak at -0.55 V , which do not vary with scanning rate, and the peak-to-peak separation ($\Delta E_{\text{p}} = E_{\text{pa}} - E_{\text{pc}}$) of 100 mV indicates a reversible one-electron reaction which may be assigned to Mn(III)/Mn(II) ($E_{1/2} = -0.6 \text{ V}$) [16]. As the peak heights for the two pairs of redox waves are similar, the redox couple at $+0.32 / +0.25 \text{ V}$ may be attributed to another one-electron process Mn(IV)/Mn(III) ($E_{1/2} = 0.29 \text{ V}$).

Our CV results are in agreement with those of the effective mimic transition-metal complexes having similar SOD activities reported in the literature [16–18].

Supplementary Materials

Tables of x-ray crystallographic data in CIF format for the structures reported in this paper have been deposited with the Cambridge Crystallographic Data Centre as supplementary publications CCDC 153172–153174. Copies of the available material can be

obtained, free of charge, on application to CCDC, 12 Union Road, Cambridge CB2 1EZ, U.K. (e-mail: deposit@ccdc.cam.ac.uk).

Acknowledgements

This work was financially supported by the National Natural Science Foundation of China (No. 29625102 & 29625102). We also thank the Chemistry Department of the Chinese University of Hong Kong for donation of the diffractometer.

References

- [1] J.V. Bannister, W.H. Bannister and G. Rotilio (1987). *Crit. Rev. Biochem.*, **22**, 11.
- [2] J.M. McCord and I. Fridovich (1969). *J. Biol. Chem.*, **244**, 6049.
- [3] D.P. Riley and R.H. Weiss (1994). *J. Am. Chem. Soc.*, **116**, 387.
- [4] R. Rajan, R. Rajaram, B.U. Nair, T. Ramasami and S.K. Mandal (1996). *J. Chem. Soc., Dalton Trans.*, 2019.
- [5] J.S. Valentine and D.M. de Freitas (1985). *J. Chem. Educ.*, **62**, 990.
- [6] T. Takabatake, M. Hasegawa, T. Nagano and M. Hirobe (1992). *J. Biol. Chem.*, **267**, 4613.
- [7] N. Kitajima, M. Osawa, N. Tamura, Y. Moro-oka, T. Hirano, M. Hirobe and T. Nagano (1993). *Inorg. Chem.*, **32**, 1879.
- [8] K.A. Campbell, E. Yikilmaz, C.V. Grant, W. Gregor, A.-F. Miller and R.D. Britt (1999). *J. Am. Chem. Soc.*, **121**, 4714.
- [9] M. Baudry, S. Etienns, A. Bruce, M. Palucki, E. Jacobson and B. Malfrog (1993). *Biochem. Biophys. Res. Commun.*, **192**, 964.
- [10] D.P. Riley and R.H. Weiss (1994). *J. Am. Chem. Soc.*, **116**, 387.
- [11] I. Fridovich (1985). In: R.A. Greenwald (Ed.), *CRC Handbook of Methods for Oxygen Radical Research*, p. 51. CRC, Boaz Raton, FL.
- [12] A.C.T. North, D.C. Phillips and F.S. Mathews (1968). *Acta Crystallogr., Sect. A*, **24**, 351.
- [13] G.M. Sheldrick (1997). *SHELXS-97*, Program for Crystal Structure Determination. University of Göttingen, Germany.
- [14] G.M. Sheldrick (1997). *SHELXL-97*, Program for Crystal Structure Refinement. University of Göttingen, Germany.
- [15] *International Tables for Crystallography*, Vol. C, Tables 4.2.6.8 and 6.1.1.4, (1992). Kluwer Academic Publishers, Dordrecht.
- [16] D.F. Xiang, C.Y. Duan, X.S. Tan, Q.W. Hang and W.X. Tang (1998). *J. Chem. Soc., Dalton Trans.*, 1201.
- [17] N. Kitajima, M. Osawa, N. Tamura, Y. Mora-lia, T. Hirano, M. Hirobe and T. Nagano (1993). *Inorg. Chem.*, **32**, 1879.
- [18] Z.-R. Liao, W.-Q. Liu, J.-P. Liu, Y.-Q. Jiang, J. Shi and C.-L. Liu (1994). *J. Inorg. Biochem.*, **55**, 165.